Online Available at: https://www.sciplatform.com/index.php/ijcrt/article/view/1277

ISSN (Online) = 2707-5218

International Journal of Cotton Research and Technology

Research Manuscript https://www.sciplatform.com/index.php/ijcrt

Investigation of predictability of cotton plant production area soil moisture and temperature values with SAR and optical satellite images

Serkan Kiliçaslan [a], Remzi Ekinci [a], Mehmet Cengiz Arslanoğlu [b]

[a] Faculty of Agriculture, Department of Field Crops, Dicle University,

[b] Faculty of Engineering and Architecture, Department of Computer Engineering, Batman University

*Corresponding Author's Email Address: serkankilicaslan@hotmail.com

Review Proccess: Peer review

ABSTRACT

In the study carried out in 8 villages and 27 cotton parcels in the Artuklu and Kızıltepe Districts of Mardin Province, data logger devices were installed on the lands. These devices are programmed to record soil temperature and humidity values every 6 hours. The data collected from the data loggers were compared with the Landsat-8 and Sentinel-1 images used by pre-processing in the Google Earth Engine (GEE) cloud environment, and the relationship between them was investigated by analyzing them. A significant and high correlation was found between soil moisture (TN) and Sentinel-1 values, VV (R^2 = 0.67), VV-VH (R^2 =0.65), and Landsat-8 SMI (R^2 = 0.85) values. A significant and high correlation was found between soil temperature (TS) and the Sentinel-1 values of VV (R^2 = 0.57), VV-VH (R^2 =0.54), and Landsat-8 SMI (R^2 = 0.75). In conclusion, it is recommended that the Sentinel-1 VV and VV-VH bands and the Landsat-8 SMI index could be used in soil moisture (TN) and soil temperature (TS) estimation studies, while the Landsat-8 LST band is recommended to be used in larger-scale land areas and regions.

Keywords: Cotton, soil temperature, soil moisture, sar, google earth engine.

INTRODUCTION: Cotton is a raw material for many industrial sectors, such as textiles, oil, feed, chemistry, etc. While the demand for cotton products increases with the rapid population growth, it is observed that cotton production has not increased sufficiently, trade has decreased, and stocking has increased due to reasons such as the COVID-19 crisis, climate change, excessive and irregular rainfall, as well as the regional drought disaster that has started to be experienced more frequently in recent years. According to 2022 production season data, the cotton cultivation area in the world is 33.18 million ha, the production amount is 25.73 million tons, consumption is 25.62 million tons, and the stock amount is 20.45 million tons. In Turkey, the cotton cultivation area is 480000 ha, the production is 833.000 tons, the consumption is 1.61 million tons, and the stock is 1.54 million tons. The cotton plant has a vegetation period of 170-185 days, and the annual water requirement is between 492 and 1153 mm, with an average of 700-800 mm in our country. In regions where there is little rainfall between April and October, which is the growing season of cotton, especially in the Mediterranean and south-eastern Anatolia, the water deficit is tried to be filled with irrigation. This can be a problem in terms of consumption of natural resources, the environment, and soil, as well as increasing the need for energy and labour, which comes to the fore in terms of production costs. Therefore, an effective irrigation method with irrigation at the right time and amount is very important. In addition to various classical measurement and evaluation methods in these subjects, remote sensing technology, as a relatively new technology, also emerges. Remote sensing is the science and art of measuring and determining the properties of an object by interpreting the electromagnetic rays reflected or emitted from the object without any physical contact with the earth or connected sources in terms of quality and quantity. Remote sensing is classified as active or passive sensing according to the type of sensor. The perception of the reflection of the rays emitted by the earth and objects themselves or from the sun is called passive, and the perception of the reflected rays by the satellite itself by sending rays to the earth is called active systems. Examples of passive systems are optical, thermal, and microwave sensors; active systems are LIDAR (light detection and ranging) and RADAR (radio detection and ranging) systems. Remote sensing is used in many areas such as vegetation cover and distribution, land use, plant growth, yield estimation, classification, and soil and plant characteristics in agriculture (Sunar et al., 2016). For some uses, plant, land, and product evaluation information is needed. For this purpose, various tools and sensors related to plant development and plant and soil structure are used. With the use of in-field sensors, soil and plant conditions are observed, and irrigation suggestions are made (Acar *et al*., 2020; El Ghandour *et al*., 2019; Koçak, 2002; Mthandi *et al*., 2013; Raper, 2014), The effect of meteorological events is also observed (Aktaş & Üstündağ, 2020). The two situations were combined and the relationship between them was tried to be determined (Bulut et al., 2019). Soil moisture sensing performance was examined with satellite images (Serrano, 2010), global-scale evapotranspiration was determined (Zheng et al., 2017), and crop water requirements were tried to be estimated (Akdim *et al*., 2014).

OBJECTIVE: This study was carried out with the aim of recording the soil moisture and temperature values with the sensors in the cotton plant production area to the data logger device, to determine the relationships between these values and the SAR and optical satellite images, and to investigate the usability of the satellite images in estimating the humidity and temperature values.

MATERIAL AND METHODS: **Trial area:** The research was carried out in 8 villages and 27 different cotton planted plots in Mardin Province's Artuklu and Kızıltepe districts. Information about the parcels is given in figure 1 and table 1.

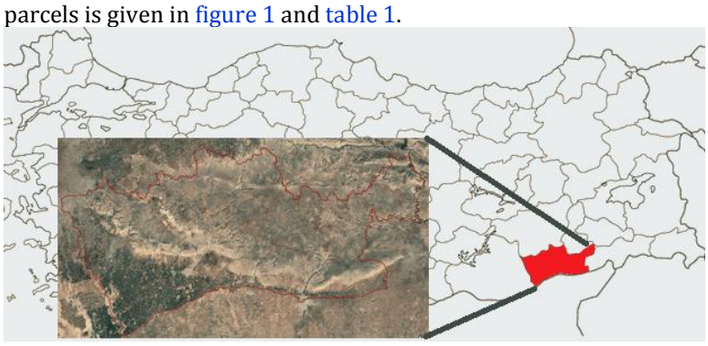

Figure 1: Information about the parcels.

NO	Village (Parcels),	X ; Y Koord.	NO	Village (Parcels),	X ; Y Koord.
S01	ALAKUŞ (133/1)	40,856; 37,139	S15	ALTINTOPRAK (113/1)	40,611; 7,100
S02	ALAKUŞ (133/1)	40,860; 37,138	S16	ALTINTOPRAK (117/1)	40,596; 37,1
S03	ALAKUŞ (116/6)	40,878; 37,142	S17	TANRIVERDİ (135/1)	40,583; 7,094
S04	ALAKUŞ (130/1)	40,866; 37,136	S18	TANRIVERDİ (134/1)	40,578; 37,097
S05	ALAKUŞ (130/2)	40,865; 37,134	S19	ALTINTOPRAK (122/2)	40,597; 37,109
S06	KÜÇÜKKÖY (111/3)	40,853; 37,129	S20	TANRIVERDİ (113/1)	40,591; 37,067
S07	ALAKUŞ (116/3)	40,877; 37,157	S21	TANRIVERDİ (110/3)	40,590; 37,075
S08	ÇIPLAKTEPE (108/11)	40,843; 37,52	S22	AKYÜZ (109/2)	40,531; 37,108
S09	ÇIPLAKTEPE (108/4)	40,846; 37,157	S23	AKYÜZ (108/6)	40,538; 37,113
S10	DİBEKTAŞ 116/13)	40,836; 37,128	S24	AKYÜZ (122/1)	40,565; 37,112
S11	DİBEKTAŞ (116/12)	40,834; 37,128	S25	AKYÜZ (101/4)	40,549; 37,114
S12	ALTINTOPRAK (103/1)	40,598; 37,119	S26	GÖZLÜCE (107/2)	40,531; 37,072
S13	ALTINTOPRAK (103/1)	40,593; 37,124	S27	GÖZLÜCE (107/3)	40,528; 37,073
S14	ALTINTOPRAK (102/1)	40,600; 37,114			

Table 1: Information and coordinates of the parcels.

The cotton plant was planted in 2021 in the study areas, and in-farm cultural processes, maintenance feeding, and irrigation processes were carried out under farmer conditions, and no additional applications were made. During the June-September period in which the study was conducted, no precipitation occurred in the region. Changes in temperature and humidity values during the vegetation period are given in figure 2.

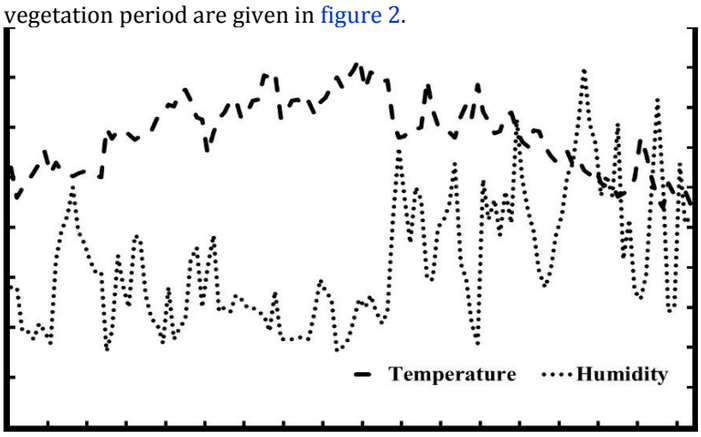

 Digital Object Identifier: https://dx.doi.org/10.33865/ijcrt.006.01.1277

Figure 2: Change in temperature and humidity values during the vegetation period.

Data Logger: Within the scope of the research, 27 data logger devices were used, and the data read by the ambient humidity and temperature sensors and the soil moisture and temperature sensors were obtained. The devices are programmed with the Arduino software program and are programmed to record one value every six hours. The data logger is given in figure 3 a-d.

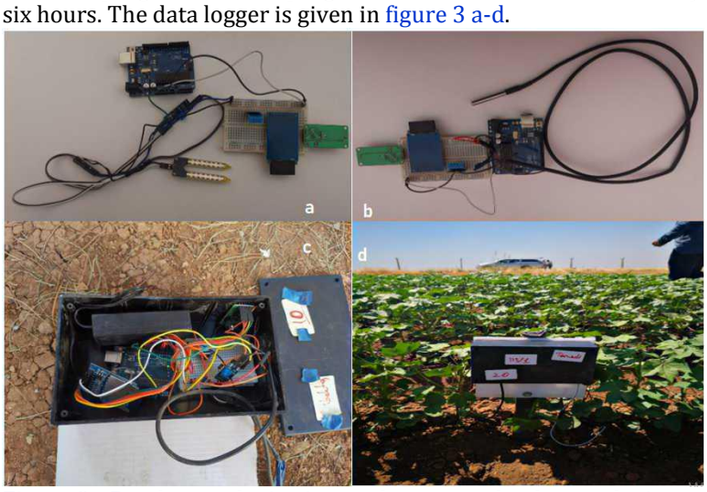

Figure 3 : Datalogger device internal parts, c:, datalogger device as mounted, d: field use of the datalogger device

Soil Moisture (TN) and temperature (TS) sensor features: Temperature was measured with ±0.1 °C accuracy between 0 and +300 °C, and humidity was measured between 0 and 100% with ±5% humidity accuracy. The devices were installed in the field in the 2nd week of June, and the data were collected in the first week of September. During this period, the devices recorded the soil moisture (TN) and soil temperature (TS) values in the field.

Sentinel-1: Within the framework of the Copernicus Program carried out by the European Space Agency (ESA), the first (Sentinel-1 A) was launched in 2014, and the second (Sentinel-1 B) was launched in 2016. It has a C-band synthetic aperture radar (SAR) sensor with spatial resolution up to 5*20 meters, VV, VH dual polarization as vertical (V) and horizontal (H) (Anonymous, 2023a). Sentinel-1 interferometry ground range detected (GRD) level images were used in the study (figure 4).

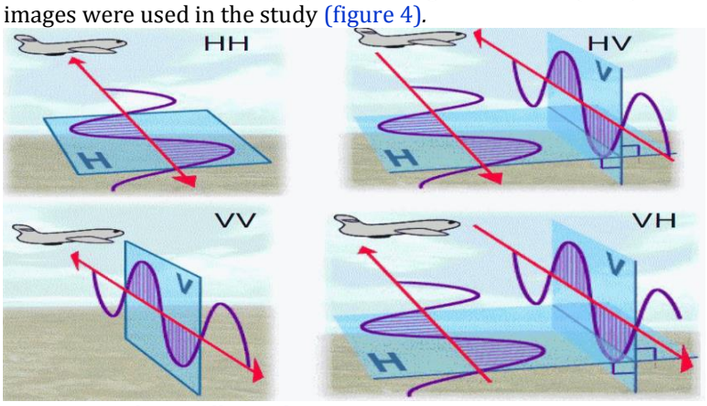

Figure 4: Radar satellite polarizations.

Sentinel-1 Refined Lee, Gamma Map, and Perona Malik (Cresson *et al.*, 2018; Mansourpour *et al.*, 2006; Medasani & Reddy, 2017) filters were used for speckle filtering in GRD images. Refined Lee filter takes the average of the determined area while preserving the edges, providing better preservation of image details (Medasani & Reddy, 2017). Gamma Map filter assumes that the scene reflectivity is a Gaussian distribution while preserving the high-frequency features (Mansourpour *et al.*, 2006). The Perona Malik filter is used to soften images while preserving the contours of objects (Cresson *et al.*, 2018). These filters were also used in the GEE environment, and the band values obtained were processed into the MS Office Excel program.

Landsat-8: It was launched by the United States Geological Society (USGS) in 2013 and includes a 15-30 m resolution Operational Terrain Imager (OLI) and a 100 m resolution Thermal Infrared Sensor (TIRS). Landsat-8 land surface reflection (SR) images were used in the study.

Normalized difference crop index (NDVI): It was used to evaluate changes in plant growth and plant health. The ratio between the red and near infrared bands (Rouse *et al.*, 1973), determined by the equation 1.

NDVI = (NIR-RED)/(NIR+RED)

Black surface temperature (LST): The top of Atmosphere Reflectance (TOA) algorithm converts Landsat-8 thermal band (Band 10) pixel digital numbers to luminance temperature (Cohen *et al.*, 2021). Using this transformed band, the surface temperature of the land is calculated in figure 5 (Avdan & Jovanovska, 2016).

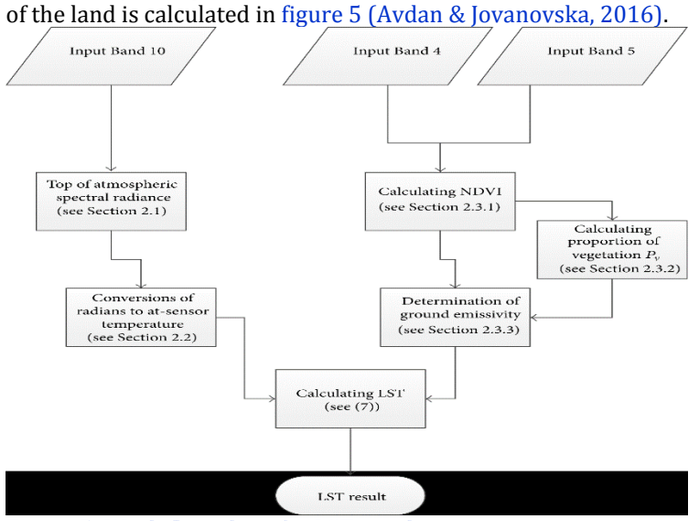

Figure 5: Work flow chart for LST purchase.

Soil moisture index (SMI): It was developed for soil moisture estimation using NDVI and LST values for Landsat series satellites. SMI is determined by the equation 2 (Zeng *et al.*, 2004).

SMI = (LST_max–LST)/(LST_max-LST_min)

Google earth engine (GEE): Introduced by Google in 2010. It is a cloud-based geospatial computing platform. Data storage, analysis, and production of outputs and maps in various formats, as well as being able to operate on a regional, national, and global scale, provide great advantages for users. Sentinel-1 and Landsat-8 satellite images were obtained over the GEE environment. In this platform, trajectory correction, corner noise removal, thermal noise removal, radiometric calibration, and terrain correction operations have been performed as part of the pre-processing for Sentinel-1 GRD images, and geometric, radiometric, and atmospheric correction operations using the Land Surface Reflectance Code (LaSRC) algorithm for Landsat-8 images have also been performed. Band pixel values obtained by determining the time intervals were processed into the MS Office Excel program and subjected to variance analysis in the JMP 5.0.1 (Copyright © 1989–2002 SAS Institute Inc.) statistical program with DL values (figure 6).

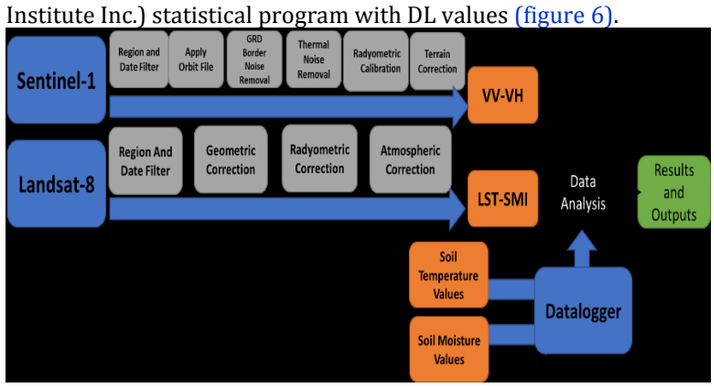

Figure 6: Workflow protocol

RESULTS AND DISCUSSIONS: First, correlation analysis was done on TN and TS data from data loggers and the Sentinel-1 and Landsat-8 satellites. Then, regression analysis was done on the data that was statistically significant. The regression analysis results of the TN data obtained are given in table 1, and the regression and reverse regression analysis results of the TS data are given in table 2.

Band/İndex	R^2	RMSE	Regression Equation	Regression Equation
VV	**0.67****	**0.03**	**Y= 0,00274*TN + 0,06823**	**Y= 246.09*VV-4.54**
VH	0.06**	0.01	Y =0.00013*TN + 0.02565	Y = 406.18*VH + 25.09
VV-VH	**0.65****	**0.03**	**Y = 0,00260*TN + 0,04258**	**Y = 249.47*VV-VH + 2.53**
LEE_VH	0.08**	1.41	Y =0.02356*TN-16.36457	Y = 3.41*LEE_VH + 90.31
LEE_VV	0.61**	0.86	Y = 0.06108*TN-10.28835	Y = 10.02*LEE_VV + 117.62
GAMMA_VH	0.11**	1.24	Y = 0.02314*TN-16.26267	Y = 4.23*GAMMA_VH + 102.68
GAMMA_VV	0.56**	0.82	Y = 0.05167*TN-9.80801	Y = 10.75*GAMMA_VV + 122.14
MALIK_VH	0.08**	1.51	Y = 0.02439*TN-16.431	Y = 3.08*MALIK_VH + 85.36
MALIK_VV	0.63**	0.87	Y = 0.06409*TN-10.41644	Y = 9.79*MALIK_VV + 115.94
SMI	**0.85****	**0.10**	**Y = 0.01*TN - 0.02**	**Y = 77.76*SMI + 9.87**
LST	0.34**	4.18	Y =-0.13210*TN+ 44.39125	Y = 2.60*LST- 151.97

Table 2: Soil Moisture (TN) Data and Sentinel-1 and Landsat-8 band/indices regression/inverse regression analysis results.

 Digital Object Identifier: https://dx.doi.org/10.33865/ijcrt.006.01.1277

TN: Soil Moisture, R^2: Regression Coefficient, RMSE: Root Means Squared Error, **:0.01 significant

It is seen that there is a linear (y = 0.00274 TN + 0.06823) (R^2=0.67) relationship between soil moisture (TN) and Sentinel-1 VV band values (table 1 and figure 7). The existence of a linear and significant (1%) relationship between soil moisture and Sentinel-1 VV band values reveals that it can be used to determine instantaneous or dynamic soil moisture values and Sentinel-1 VV band values. It is seen that there is a linear (y = 246.09*VV + -4.54) (R^2=0.67) relationship between Sentinel-1 VV band values and soil moisture (TN) (table 2 and figure 7). The existence of a linear and significant (1%) relationship between Sentinel-1 VV band values and soil moisture reveals that Sentinel-1 VV band values can be used to determine soil moisture values. It is seen that there is a linear (y = 0.00260 TN+0.04258) (R^2=0.65) relationship between soil moisture (TN) and Sentinel-1 VV-VH band values (table 1 and figure 8).

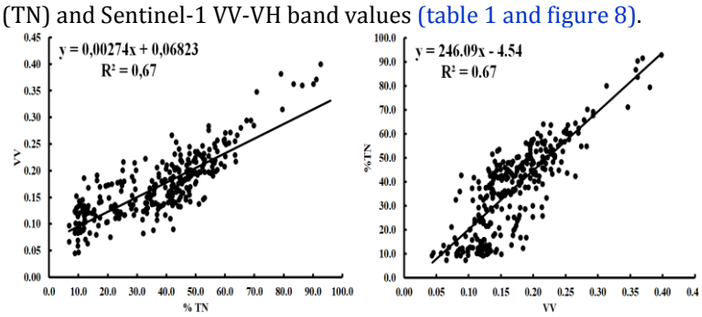

Figure 7: Change between VV and Soil Moisture (TN).

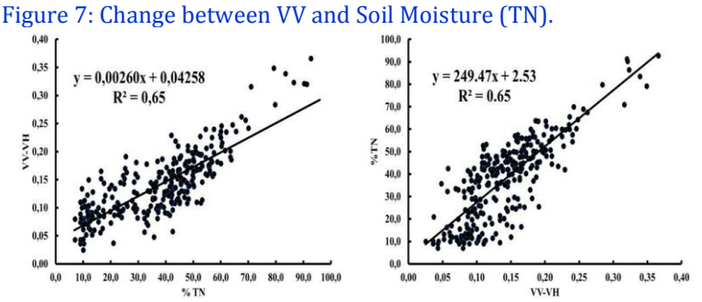

Figure 8: Change between VV-VH and Soil Moisture (TN).

The existence of a linear and significant (1%) relationship between soil moisture and Sentinel-1 VV-VH band values reveals that it can be used to determine instantaneous or dynamic soil moisture values and Sentinel-1 VV-VH band values. It is seen that there is a linear (y = 249.47*VV-VH + 2.53) (R^2=0.65) relationship between Sentinel-1 VV-VH band values and soil moisture (TN) (table 2 and figure 8). The existence of a linear and significant (1%) relationship between Sentinel-1 VV-VH band values and soil moisture reveals that Sentinel-1 VV-VH band values can be used to determine soil moisture values. Our findings, obtained between VV, VV-VH bands, and TN, are based on study to predict annual soil water content in vegetated lands with the help of SAR images and machine learning techniques; soil moisture satellite data are promising to increase the reliability of flood measures (Ahlmer *et al*., 2018). The Sentinel-1 VV band showed a better relationship than the VH band in estimating soil moisture with the help of Sentinel-1 microwave and Landsat 7/8 thermal data (Amazirh *et al*., 2019); evaluating the use of active and passive data separately and together in obtaining soil moisture information, (Amer *et al*., 2011); (Bauer-Marschallinger *et al*., 2018), reporting that Sentinel-1 data are highly productive in plains, forests, and agricultural areas. Development a remote sensing product combining active and passive microwave sensors to determine soil moisture deficits (Hirschi *et al*., 2014). Hoskera *et al*., (2020) produced various linear and generalized models by using Sentinel-1 images for volumetric soil moisture estimation; Khabbazan *et al.* (2019), who stated that Sentinel-1 data can provide reliable information in cloudy conditions in their studies for product development monitoring, Navarro *et al*. (2016), stated that Sentinel-1A data can be used with complementary and optical images in their studies for land cover monitoring in different agricultural conditions; Pablos *et al*., (2016); Schmugge *et al*., (1976), reported that microwave radiometers mounted on truck, aircraft, and spacecraft platforms are sensitive to soil moisture changes for different conditions in light or medium vegetated areas; In the study conducted for soil moisture estimation with ALOS-2 and Sentinel-1 data, Şekertekin, (2018), who stated that L-band was more effective than C-band, supports the findings.

The regression results obtained from the Refined Lee, Gamma Map, and Perona Malik filter results applied to the VV/VH band were not explained as they were lower than the regression results obtained from the VV/VH band values.

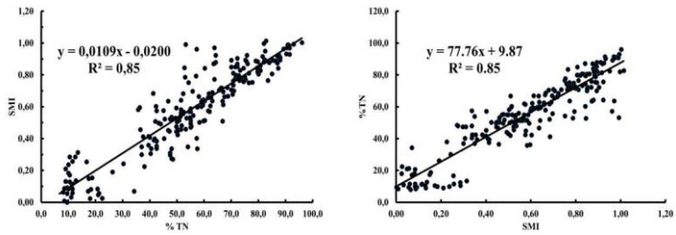

Figure 9: Change between SMI and Soil Moisture (TN).

It is seen that there is a linear (y = 0.0109*TN- 0.02) (R^2=0.85) relationship between soil moisture (TN) and the Landsat-8 SMI index (table 1 and figure 9). The existence of a linear and significant (1%) relationship between the soil moisture and the SMI value reveals that it can be used to determine the instantaneous/dynamic soil moisture value and the SMI value. It is seen that there is a linear (y = 77.76*SMI + 9.87) (R^2=0.85) relationship between the Landsat-8 SMI index and soil moisture (TN) (table 1 and figure 9). The existence of a linear and significant (1%) relationship between the Landsat-8 SMI index and soil moisture reveals that it can be used to determine the soil moisture value by determining the Landsat-8 SMI index value. Our research shows that LST data has a lot of potential for estimating soil moisture in places with little or no vegetation. Masoud *et al.* (2019); Özelkan *et al*. (2014) stated that Landsat-7 thermal images are suitable to explain the relationship between monthly average land surface temperature and air temperature, total precipitation, and relative humidity; Qui, (2006); Saha *et al*. (2018) stated that SMI derived from Landsat images can be used efficiently in the assessment of flood disasters and agricultural droughts; Stating that thermal data can be used in surface soil moisture estimation studies in their study to determine the relationship between remote sensing data and soil moisture, Syed & Javed, (2015) stated that this supports the findings of Zhang & Zhou, (2016) reported that combinations of optical and thermal images provide useful information for soil moisture estimation.

Band/İndex	R^2	RMSE	Regression Equation	Regression Equation
VV	**0.57****	**0.03**	**Y = -0,00834 TS + 0,46170**	**Y = 67.82*VV- 46.44**
VH	0.06**	0.01	Y =-0.00046*TS + 0.04669	Y = 127.06*VH - 38.74
VV-VH	**0.54****	**0.04**	**Y =-0.00788*TS + 0.41501**	**Y =-68.27*VV-VH + 44.42**
LEE_VH	0.09**	1.40	Y =- 0.08260*TS-12.60213	Y = 1.08*LEE_VH- 18.12
LEE_VV	0.54**	0.93	Y =- 0.19136*TS-1.32834	Y = 2.84*LEE_VV- 12.16
GAMMA_VH	0.11**	1.23	Y =- 0.08009*TS-12.60348	Y = 1.32*GAMMA_VH-14.46
GAMMA_VV	0.49**	0.87	Y =- 0.16191*TS-2.22716	Y = 3.06*GAMMA_VV-10.87
MALIK_VH	0.09**	1.51	Y =- 0.08559*TS-12.53337	Y = 0.98*MALIK_VH- 19.67
MALIK_VV	0.56**	0.94	Y =- 0.20116*TS-1.001942	Y = 2.78*MALIK_VV- 12.60
SMI	**0.75****	**0.13**	**Y = -0.04*TS + 1.74**	**Y = 19.92*SMI - 42.38**
LST	0.30**	4.33	Y = 0.44906*TS + 23.27058	Y = 0.66*LST + 6.15

Table 3: Soil Temperature (TS) Data and Sentinel-1 and Landsat-8 band/indices regression/ reverse regression analysis results

TS: Soil Temperature, R^2: Regression Coefficient, RMSE: Root Square Mean Error, Significant at the **:0.01 level.

It is seen that there is a linear (y = -0.00834*TS + 0.46170) (R^2=0.57) relationship between soil temperature (TS) and Sentinel-1 VV band values (table 3 and figure 10).

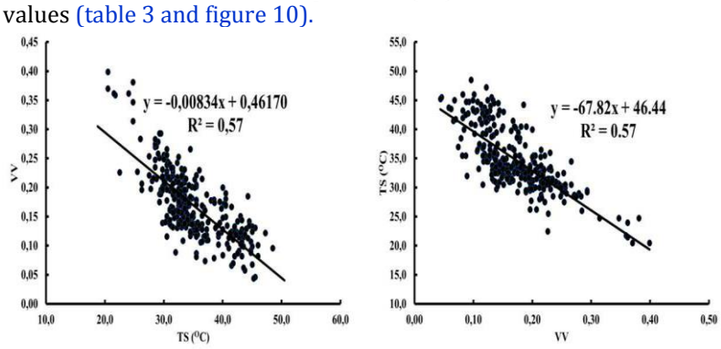

Figure 10: Change between VV and Soil Temperature (TS).

The existence of a linear and significant (1%) relationship between soil temperature and Sentinel-1 VV band values reveals that it can be used to determine instantaneous/dynamic soil temperature values and Sentinel-1 VV band values. It is seen that there is a linear (y = -67.82*VV + 46.44) (R^2=0.57) relationship between Sentinel-1 VV band values and soil temperature (TS) (table 2 and figure 10). The existence of a linear and significant (1%) relationship between Sentinel-1 VV band values and soil temperature reveals that

 Digital Object Identifier: https://dx.doi.org/10.33865/ijcrt.006.01.1277

Sentinel-1 VV band values can be used to determine soil temperature values.

It is seen that there is a linear (y = -0.00788*TS + 0.41501) (R^2=0.54) relationship between soil temperature (TS) and Sentinel-1 VV-VH band values (table 2 and figure 11).

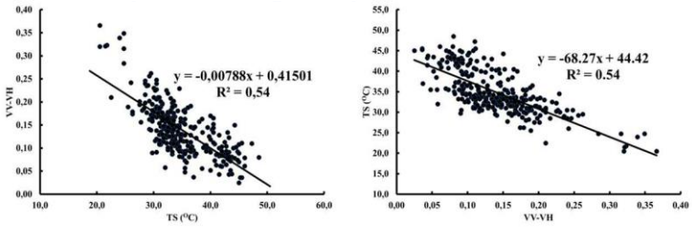

Figure 11. Change between VV-VH and soil temperature (TS).

The existence of a linear and significant (1%) relationship between the soil temperature and Sentinel-1 VV-VH band values reveals that it can be used to determine the instantaneous or dynamic soil temperature value and to determine the Sentinel-1 VV-VH band values. It is seen that there is a linear (y = -68.27*VV-VH + 44.42) (R^2=0.54) relationship between Sentinel-1 VV-VH band values and soil temperature (TS) (Table 2 and Figure 11). The existence of a linear and significant (1%) relationship between Sentinel-1 VV-VH band values and soil temperature reveals that Sentinel-1 VV-VH band values can be used to determine soil temperature values.

Our analysis findings obtained between the VV band, the VV-VH band, and the TS support the findings of (Cohen *et al*. (2021); Fayad *et al*. (2020) and Pablos *et al*. (2016). Stating that Sentinel-1 data was used to improve medium resolution MODIS land surface temperature data, Amazirh *et al*. (2019) and Rodionova (2017) reported that there is a high correlation between Sentinel-1 radar images and soil temperature. Mattia *et al*., (2017) developed a soil moisture estimation algorithm using Sentinel-1 images. The regression results obtained by applying the Refined Lee, Gamma Map, and Perona Malik filters to the VV/VH band are not explained because they are lower than the regression results obtained from the VV/VH band values.

It is seen that there is a linear (y = -0.04*TS + 1.74) (R^2=0.75) relationship between soil temperature (TS) and the Landsat-8 SMI index (table 2 and figure 12).

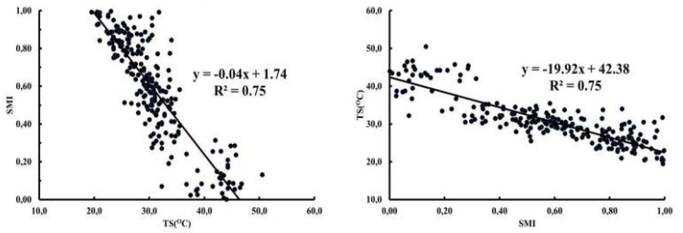

Figure 12. Change between SMI and soil temperature (TS)

The existence of a linear and significant (1%) relationship between the soil temperature and the SMI value reveals that it can be used to determine the instantaneous/dynamic soil temperature value and the SMI value. It is seen that there is a linear (y = 19.92*SMI - 42.38) (R^2=0.84) relationship between the Landsat-8 SMI index and soil temperature (TS) (table 2 and figure 12). The existence of a linear and significant (1%) relationship between the Landsat-8 SMI index and the soil temperature reveals that it can be used to determine the soil temperature value by determining the Landsat-8 SMI index value. Our findings show that Sentinel-1 VV band showed a better correlation than VH band in estimating soil moisture with the help of Sentinel-1 microwave and Landsat7/8 thermal data, Amazirh *et al*. (2018); Masoud *et al*. (2019); Özelkan *et al*. (2014) stated that Landsat-7 thermal images are suitable to explain the relationship between monthly average land surface temperature and air temperature, total precipitation, and relative humidity; (Qui, 2006) It supports the findings of Saha *et al*. (2018) stated that SMI derived from Landsat images can be used efficiently in the assessment of flood disasters and agricultural drought

CONCLUSIONS: It was observed that only the irrigation status affected the soil moisture values. There was no precipitation throughout the season, and air humidity did not affect soil moisture. Soil moisture values changed according to the irrigation situation in the field, started to rise with the start of irrigation, reached their maximum values, followed a stagnant course after the end of irrigation, and then started to decrease. The values for soil moisture, Sentinel-1 VV band, and Landsat-8 SMI index were found to have a strong and significant correlation. Soil temperature values were affected by air temperature at the beginning of the production season, when the plant mass was low, but the main factor was irrigation. It was observed that it was negatively affected by the irrigation situation; the temperature decreased from the beginning of the irrigation, the temperature values did not change much as the irrigation continued, and the soil temperature gradually increased after the irrigation was finished. A significant and high correlation was found between soil temperature values and Sentinel-1 VV band values, and a significant but low correlation was found between Landsat-8 LST values. It is thought that the reasons for the low correlation with the LST band may be due to soil covering due to the plant development period and the low (100 m) LST band resolution. Due to the low resolution, it is recommended to use this band in larger scale areas (village-district-region). According to the results of the regression analysis between soil moisture/temperature data and Sentinel-1 and Landsat-8 values; it is recommended that the Sentinel-1 VV band and Landsat-8 SMI index can be used in soil moisture estimation studies, the Sentinel-1 VV band and Landsat SMI should be used in soil temperature estimation studies, and the Landsat-8 LST band should be used in larger scale areas and regions.

CONFLICT OF INTEREST: Author has no conflict of interest.

LIFE SCIENCE REPORTING: In current research article no life science threat was reported

ETHICAL RESPONSIBILITY: This is original research, and it is not submitted in whole or in parts to another journal for publication purpose.

INFORMED CONSENT: The author(s) have reviewed the entire manuscript and approved the final version before submission.

REFERENCE: Acar, Eve Ö. & M.S. (2020). On a yearly basis prediction of soil water content utilizing sar data: A machine learning and feature selection approach. Turkish journal of electrical engineering and computer sciences, *28*, 2316–2330.

Acar, H., Özerdem, M. S., & Acar, E. (2020). Soil moisture inversion via semiempirical and machine learning methods with full-polarization Radarsat-2 and polarimetric target decomposition data: A comparative study. IEEE Access (8, 197896–197907.

Ahlmer, A. K., Cavalli, M., Hansson, K., Koutsouris, A. J., Crema, S., & Kalantari, Z. (2018). Soil moisture remote-sensing applications for identification of flood-prone areas along transport infrastructure. Environmental earth science, 77, 533.

Akdim, N., Alfieri, S. M., Habib, A., Choukri, A., Cheruiyot, E., Labbassi, K., & Menenti, M. (2014). Monitoring of Irrigation Schemes by Remote Sensing: Phenology versus Retrieval of Biophysical Variables. Remote sens, *6*, 5815–5851.

Aktaş, F. A., & Üstündağ, B. B. (2020). Soil moisture monitoring of the plant root zone by using phenology as context in remote sensing. Journal of selected topics in applied earth observations and remote sensing, *13*, 6051–6063.

Amazirh, A., Merlin, O., & Er-Raki, S. (2019). Including Sentinel-1 radar data to improve the disaggregation of MODIS land surface temperature data. ISPRS Journal of photogrammetry and remote sensing, 150, 11–26.

Amazirh, A., Merlin, O., Er-Raki, S., Gao, Q., Rivalland, V., Malbeteau, Y., Khabba, S., & Escorihuela, M. J. (2018). Retrieving surface soil moisture at high spatio-temporal resolution from a synergy between Sentinel-1 radar and Landsat thermal data: A study case over bare soil. Remote sens. Environment, 211, 321–337.

Amer, A., Yun, Z., & Sue, N. (2011). Review and evaluation of remote sensing methods for soil-moisture estimation. SPIE reviews, *2*(1), 028001.

Avdan, U., & Jovanovska, G. (2016). Algorithm for automated mapping of land surface temperature using LANDSAT 8 satellite data. Journal of sensors, 1–8.

Bauer-Marschallinger, B., Paulik, C., Hochstöger, S., Mistelbauer, T., Modanesi, S., Ciabatta, L., Massari, C., Brocca, L., & Wagner, W. (2018). Toward global soil moisture monitoring with Sentinel-1: Harnessing assets and overcoming obstacles. IEEE transactions on geoscience and remote sensing, 57(1), 520–539.

Bulut, B., Yilmaz, M. T., Afshar, M. H., Şorman, A. Ü., Yücel, İ., Cosh, M. H., & Şimşek, O. (2019). Evaluation of Remotely-Sensed and Model-Based Soil Moisture Products According to Different Soil Type, Vegetation Cover and Climate Regime Using Station-Based Observations over Turkey. Remote sens, 11, 1875.

Cohen, J., Rautiainen, K., Lemmetyinen, J., Smolander, T., Vehviläinen, J., & Pulliainen, J. (2021). Sentinel-1 based soil freeze/thaw estimation in boreal forest environments. Remote sensing of environment, *254*, 112267.

Cresson, R., Grizonnet, M., & Michel, J. (2018). Orfeo ToolBox Applications. QGIS and generic tools, 1, 151–242.

El Ghandour, F.-E., Alfieri, S. M., Houali, Y., Habib, A., Akdim, N., Labbassi, K., & Menenti, M. (2019). Detecting the Response of Irrigation Water Management to Climate by Remote Sensing Monitoring of Evapotranspiration. Water, 11.

Fayad, I., Baghdadi, N., Bazzi, H., & Zribi, M. (2020). Near real-time freeze detection over agricultural plots using Sentinel-1 data. Remote sensing, 12(12).

Hirschi, M., Mueller, B., Dorigo, W., & Seneviratne, S. I. (2014). Using remotely sensed soil moisture for land–atmosphere coupling diagnostics: The role of surface vs. Root-zone soil moisture variability. Remote sensing of environment,volume, *154*, 246-252,.

Hoskera, A. K., Nico, G., Irshad Ahmed, M., & Whitbread, A. (2020). Accuracies of Soil Moisture Estimations Using a Semi-Empirical Model over Bare Soil Agricultural Croplands from Sentinel-1 SAR Data. Remote sens, *12*, 1664.

Khabbazan, S., Vermunt, P., Steele-Dunne, S., Ratering Arntz, L., Marinetti, C., Valk, D., Iannini, L., Molijn, R., Westerdijk, K., & Sande, C. (2019). Crop Monitoring Using Sentinel-1 Data: A Case Study from The Netherlands. Remote sens, *11*, 1887.

Koçak, M. (2002). Elektriksel yöntemlerle algılanan toprak neminin sulama otomasyonunda kullanılması Ankara Üniv. İn Fen Bilimleri Enstitüsü Tarım Makinaları Anabilim Dalı Doktora Tezi.

Mansourpour, M., Rajabi, M. A., & Blais, J. A. R. (2006). Effects and performance of speckle noise reduction filters on active radar and SAR images. Process isprs, 36(1), 41.

Masoud, G., Mohammad, R. M., & Meisam, A. (2019). Soil moisture estimation using land surface temperature and soil temperature at 5 cm depth. International journal of remote sensing, 40(1), 104–117.

Mattia, F., Balenzano, A., Satalino, G., Lovergine, F., Loew, A., Peng, J., Wegmuller, U., Santoro, M., Cartus, O., & Dabrowska-Zielinska, K. (2017). Sentinel-1 high resolution soil moisture. Proceedings of the IEEE International Geoscience and Remote Sensing Symposium (IGARSS, 5533–5536.

Medasani, S., & Reddy, G. U. (2017). Analysis and evaluation of speckle filters for polarimetric synthetic aperture radar (PolSAR) data. International journal of applied engineering research, 12(15), 4916–4927.

Mthandi, J., Kahimba, F., Tarimo, A., Salim, B., & Lowole, M. (2013). Root zone soil moisture redistribution in maize (Zea mays L.) under different water application regimes. Agricultural sciences, 4, 521–528.

Navarro, A., Rolim, J., Miguel, I., Catalão, J., Silva, J., Painho, M., & Vekerdy, Z. (2016). Crop Monitoring Based on SPOT-5 Take-5 and Sentinel-1A Data for the Estimation of Crop Water Requirements. Remote sens, 8, 525.

Özelkan, E., Bagis, S., Ozelkan, C. E. ve Ü., & B.B. (2014). Land surface temperature retrieval for climate analysis and association with climate data. European journal of remote sensing, 655–669.

Pablos, M., Martínez-Fernández, J., Piles, M., Sánchez, N., Vall-llossera, M., & Camps, A. (2016). Multi-Temporal Evaluation of Soil Moisture and Land Surface Temperature Dynamics Using in Situ and Satellite Observations. Remote sens, *8*, 587.

Qui, H. (2006). *Rhermal remote sensing of soil moisture: Validation of presumed linear relation between surface temperature gradient and soil moisture content*. The University of Melbourne, Civil and Environmental Engineering Department, A final year research Project.

Raper, T. B. (2014). *In-season drought monitoring: Testing instrumentation and developing methods of measurement analysis*. University of Arkansas.

Rodionova, N. V. (2017). Sentinel-1 Data Correlation with Ground Measurements of Soil Temperature. *Sovremennye Problemy Distantsionnogo Zondirovaniya Zemli Iz Kosmosa*, *14*(5), 135–148.

Rouse Jr, J. W., Haas, R. H., Schell, J. A., & Deering, D. W. (1973). *Monitoring the vernal advancement and retrogradation (green wave effect) of natural vegetation*. https://ntrs.nasa.gov/api/citations/19730017588/downloads/19730017588.pdf

Saha, A., Patil, M., Goyal, V., & Rathore, D. S. (2018). Assessment and impact of soil moisture index in agricultural drought estimation using remote sensing and gis techniques. 3rd international electronic conference on water sciences, 3.

Schmugge, T., Wilheit, T., Webster, W., & Gloersen, P. (1976). *Remote sensing of soil moisture with microwave radiometers-II*. Nasa Technical Note, Nasa TN D-8321, National aeronautics and space administration.

Şekertekin, A. İ. (2018). Aktif mikrodalga uydu görüntü verileri kullanılarak toprak neminin belirlenmesi. İn Bülent Ecevit Üniversitesi Fen Bilimleri Enstitüsü Geomatik Mühendisliği Anabilim Dalı Doktora Tezi.

Serrano, M. H. L. R. (2010). *Satellite remote sensing of soil moisture*. University of Reading, Department of Meteorology, Degree of Master of Science.

Sunar, F., Özkan, Ç. ve O., & B. (2016). *Uzaktan Algılama*. Eskişehir, Anadolu Üniversitesi.

Syed, M. Z. Y., & Javed, I. (2015). Estimation of soil moisture using multispectral and FTIR techniques. The egyptian journal of remote sensing and space science, 18, 151-161.

Zeng, Y., Feng, Z., & Xiang, N. (2004). Assessment of soil moisture using Landsat ETM+ temperature/vegetation index in semiarid environment. IGARSS 2004. 2004 IEEE International Geoscience and Remote Sensing Symposium, 6, 4306–4309.

Zhang, D., & Zhou, G. (2016). Estimation of Soil Moisture from Optical and Thermal Remote Sensing: A Review. Sensors (Basel, Switzerland, 16(8), 1308.

Zheng, C., Jia, L., Hu, G., Menenti, M., Lu, J., Zhou, J., K., W., & Li, Z. (2017). Assessment of Water Use in Pan-Eurasian and African Continents by ETMonitor with Multi-Source Satellite Data. IOP Conference Series: Earth and Environmental Science.

Except where otherwise noted, this item's licence is described as **© The Author(s) 2024**. Open Access. This item is licensed under a **Creative Commons Attribution 4.0 International License**, which permits use, sharing, adaptation, distribution and reproduction in any medium or format, as long as you give appropriate credit to the original author(s) and the source, provide a link to the Creative Commons license, and indicate if changes were made. The images or other third party material in this it are included in the article's Creative Commons license, unless indicated otherwise in a credit line to the material. If material is not included in the article's Creative Commons license and your intended use is not permitted by statutory regulation or exceeds the permitted use, you will need to obtain permission directly from the copyright holder.